Simultaneous Maximization of Char Yield and Volatility of Oil from Biomass Pyrolysis

Conversion Characteristics of Aromatic Hydrocarbons in Simulated Gaseous Atmospheres in Reducing Section of Two-Stage Entrained-Flow Coal Gasifier in Air- and O_2/CO_2-blown Modes

Yasuhiro Sakurai[a], *Shuji Yamamoto*[a], *Shinji Kudo*[b], *Koyo Norinaga*[c], *Jun-ichiro Hayashi*[*,b,c]

[a] Interdisciplinary Graduate School of Engineering Sciences, Kyushu University, Kasuga 816-8580, Japan

[b] Research and Education Center of Carbon Resources, Kyushu University, Kasuga 816-8580, Japan

[c] Institute for Materials Chemistry and Engineering, Kyushu University, Kasuga 816-8580, Japan

ABSTRACT

Conversion of refractory aromatic hydrocarbons was studied with an atmospheric flow reactor that simulated the reducing section of a two-stage entrained-flow coal gasifier in an air-blown and O_2/CO_2-blown (CO_2 recycling) modes at temperature of 1100–1400 °C. Mixed vapors

of benzene and naphthalene (7/3 on a carbon basis) were fed into the reactor at total concentration in a range from 3.7 to 37 g·Nm^{-3} together with a CO-CO_2-H_2-H_2O mixture in the O_2/CO_2-blown mode or CO-CO_2-H_2-H_2O-N_2 mixture in the air-blown mode. Soot was the major fate of the aromatics at the inlet benzene/naphthalene concentration of 35–37 g·Nm^{-3}, and its yield was not influenced significantly either by the mode of gasification or temperature at 1200–1400 °C. The contribution of gas-phase reforming to the conversion of the aromatics became more important as their inlet concentration decreased. At the inlet concentration of 3.7–7.5 g·Nm^{-3}, the O_2/CO_2-blown mode was clearly more effective in reducing the soot yield than the air-blown mode and increasing the gas yield. It was explained on the basis of a detailed chemical kinetic model that the increased partial pressure of CO_2 induced higher concentration of key active species such as hydroxyl radicals that initiated the oxidative decomposition of the aromatics.

1. Introduction

Integrated coal gasification combined cycle (IGCC) is one of the promising technologies for clean coal power generation and synthesis gas production. In Japan, an IGCC employing an air-blown gasifier has been developed at a demonstration scale.[1–4] In parallel with this, another type of IGCC that employs a mixture of CO_2 recycled from gas turbine and O_2 instead of air has been studied at laboratory and bench scales.[5–6] Changing the gasifying agent from air to an O_2/CO_2 mixture will enable to recover high purity CO_2 that is available in carbon sequestration and storage (CCS). It is also expected that the increased CO_2 concentration leads to complete

gasification of coal at lower oxygen ratio, and produces electricity with efficiency as high as 45%-HHV even with CCS.[5]

Both of the above described IGCCs adopt the same types of two-stage entrained-flow coal gasifiers as shown in Figure 1.[1–4,6] The gasifier consists of two sections; the combustion section and the reducing one that are connected through the diffuser. Pulverized coal and char recycled from the reducing section are injected into the combustion section and gasified with air or O_2/CO_2 at 1600–1800 °C that is well above ash fusion temperature. The hot gas formed in the combustion section is introduced into the reducing section, and mixed with pulverized coal, which is heated rapidly and pyrolyzed. The pyrolysis products; char and volatiles, are *in-situ* converted into gas by endothermic gasification and reforming with CO_2 and H_2O, respectively.

The overall extent of the endothermic reactions, which can be represented by the temperature of product gas at the exit of gasifier (T_{exit}), is crucial for gasifier performance because T_{exit} is a factor that determines cold gas efficiency. More extensive gasification in the reducing section and resultant lower T_{exit} are thus preferred to improve the efficiency.[7–8] However, lower T_{exit} may allow more tar, *i.e.*, aromatic compounds derived from the volatiles, to survive in and escape from the reducing section causing contamination of the synthesis gas. It is believed that H_2O and CO_2 gasification of the char are the rate-determining step, and its kinetics and mechanism have been studied extensively.[9–15] Much less, on the other hand, is known about the conversion of the volatiles,[16] which may be due to a belief of immediate and complete reforming of tar and lower hydrocarbons with H_2O and CO_2 at high temperature. Vapor-phase behavior of aromatic compounds, in particular that in gaseous atmosphere relevant to the reducing section at 1100–1400 °C, is thus important, but very little is known about it.[3,17–18]

In the present work, conversion of benzene and naphthalene as model tar compounds has been studied with a main focus on the combined effects of temperature, gaseous atmosphere and concentration of the aromatic hydrocarbons. The vapor of the aromatics was converted in a CO-CO_2-H_2-H_2O or CO-CO_2-H_2-H_2O-N_2 atmosphere in a tubular reactor to simulate the reducing section of two-stage entrained-flow coal gasifier.

2. Determination of Feed Gas Compositions

In the reducing section of the gasifier, the gas/solid suspension goes upward while cooled down to T_{exit}, with the progress of endothermic gasification and reforming of char and volatiles, respectively. An axial temperature distribution is thus created in the section with the lowest temperature, T_{exit}. In addition, the synthesis gas contains oxidizing agent, *i.e.*, H_2O and CO_2, with lowest concentrations at the exit. Here is assumed that benzene or naphthalene is converted in a plug flow and isothermal reactor at a given temperature (T_r) and in an atmosphere being equivalent with that at the gasifier exit. If complete conversion of the benzene or naphthalene is demonstrated experimentally at $T_r = T_{exit}$ and in the corresponding atmosphere, it guarantees complete conversion of the compound in the reducing section with T_{exit}. It may also be expected that the other aromatics are converted completely because benzene and naphthalene are believed to be most refractory compounds among the aromatics.[19–21]

To determine the feed gas compositions for the experiments, numerical simulation of coal gasification was performed. The gas compositions at the exit of the reducing section were estimated assuming that the overall heat loss from the gasifier (except for heat carried by the synthesis gas) was 3% of the coal's LHV, and that CO, CO_2, H_2 and H_2O were chemically

equilibrated at the exit of the reducing section. The other assumptions in the simulation are listed in Table 1.

The simulation gave the composition of the synthesis gas as well as the air or oxygen ratio, relative amount of coal fed into the reducing section to that into the combustion section and the amount of char recycled into the combustion section (*i.e.*, the conversion of the coal fed into the reducing section) as a function of T_{exit}. Validity of the numerical simulation was examined referring to previous reports on the two-stage entrained-flow gasification of coal.[22–23] The simulation predicted a cold gas efficiency of 76.0% on an LHV basis for the air-blown mode with T_{exit} = 1100 °C, which was in good agreement with those reported by Ishibashi *et al.*, 75.3%[22] and Hashimoto *et al.*, 77.2%.[23]

Table 2 shows the synthesis gas compositions predicted by the simulation for the air-blown and O_2/CO_2-blown modes, which are hereafter referred to as the air and O_2/CO_2 modes, respectively. A higher T_{exit} gives higher concentrations of CO_2 and H_2O for both modes. The concentrations of CO, CO_2, H_2 and H_2O in the air mode are clearly lower than those in the O_2/CO_2 mode due to the dilution of the air with nitrogen. The N_2 concentration is in a range of 56–60 vol% in the air mode, while that of CO ranges from 63 to 60 vol% in the O_2/CO_2 mode. The H_2O/H_2 and CO_2/CO ratios in the O_2/CO_2 mode are both higher than those in the air mode. The synthesis gas compositions shown in Table 2 were employed as those of the feed gas for the experimental runs.

3. Experimental section

Figure 2 shows a schematic diagram of the experimental apparatus. The reactor was made of nonporous mullite tube with an inner diameter of 30 mm and length of 1,800 mm. A mixture of benzene and naphthalene (7/3 on carbon basis) was continuously supplied from the syringe pump to the evaporator at room temperature and 250°C, respectively, at a constant rate. The vapor formed in the evaporator was mixed with the feed gas at a constant flow rate of 1500 $mL \cdot min^{-1}$ (25 °C and 101 kPa, on wet gas basis). The feeding rate of benzene and naphthalene was around 0.3, 0.6, or 3 $g \cdot h^{-1}$, which corresponded to the concentrations of *ca.* 4, 7 or 35–37 $g \cdot Nm^{-3}$ (0 °C and 101 kPa, on wet gas basis), respectively. The temperature of the isothermal zone of the reactor (750 mm long), *i.e.*, T_r, was maintained at 1100, 1200, 1300 or 1400 °C. The composition of the feed gas was chosen according to T_r. The gas residence time within the isothermal zone was calculated as 3.7–4.6 s in the case of no change in the chemical composition of the gas in the isothermal zone. The total concentration of benzene and naphthalene at the reactor inlet is hereafter denoted by $C_{B/N,i}$. Benzene and naphthalene will often be abbreviated as B/N.

The products from the reforming; non-condensable gas, tar, water, and soot, were introduced into the collectors, which consisted of the thimble filter made of silica fibers (150 °C), first cold trap (–70 °C), second cold trap (–70 °C) and gasbag in series. The condensable products; aromatic hydrocarbons and water, were condensed in the cold traps. The second cold trap was packed with glass beads to enhance the heat transfer and condense the vapor of water and aromatics completely. The non-condensable gases were collected in the gasbag and analyzed with Shimadzu GC-8A, GC-2014 and GC-14B gas chromatographs.

The products condensed in the cold traps were dissolved into a mixture of dichloromethane and methanol. The thimble filter and other glassware were washed with

dichloromethane, and the resultant slurry was filtered with a membrane filter (pore size; 0.45 μm) and separated into the soot and the liquid. The condensable compounds deposited on the reactor wall were washed off with dichloromethane, and the resultant slurry was filtered in the same way as described above. Aromatic compounds dissolved in the solution were detected and quantified by using a gas chromatograph (Hewlett-Packard, model HP6890) and a gas chromatography/mass spectrometer (GC/MS; PerkinElmer, model Clarus SQ 8S).

The soot deposited on the reactor wall was scratched off as much as possible, and the remaining soot was quantified by a general combustion method. The mass of the soot recovered from the reactor (soot-W) and that collected with the thimble filter (soot-F) were measured individually, and their yields were determined on the carbon basis assuming that the carbon content of the soot was 99 wt%.

4. Results and Discussion

4.1. Characteristics of B/N conversion at higher initial concentration.

Table 3 summarizes the product distributions for the air and O_2/CO_2 modes with $C_{B/N,i}$ of 35–37 $g \cdot Nm^{-3}$. The yields of the carbon containing products are indicated on a basis of B/N carbon, and also shown in Figure 3. The tar is defined as the aromatic compounds except for B/N.

At 1100 °C, the O_2/CO_2 mode gave slightly lower B/N conversion and lower soot yield but higher gas yield than the air mode. This suggested that the O_2/CO_2 mode promoted the reforming of B/N to gas while suppressed the soot formation, and also that the soot formation was faster than the reforming at 1100 °C. Table 4 shows the composition of tar. At 1100 °C, the yields of

mono- to tetra-aromatics except for acenaphthylene were higher in the O_2/CO_2 mode by 1.3 to 60 times than in the air mode. The higher yields of those aromatics, which were intermediates between B/N and gas or between B/N and soot, in the O_2/CO_2 mode than the air mode were explainable by the slower soot formation in the former mode as well as much faster soot formation than the reforming in both modes at 1100 °C. The yield of acenaphthylene was higher in the air mode by 5 times than in the O_2/CO_2 mode. It is generally accepted that acenaphthylene is formed by addition of a C_2 hydrocarbon gas (including radicals) to naphthalene or naphthyl radical.[19] Such a reaction, or otherwise, conversion of acenaphthylene was promoted in the air mode while suppressed in the O_2/CO_2 mode.

At 1200–1400 °C, the soot accounted for 2/3 or even more of the products on a basis of B/N carbon. More importantly, the soot yield seemed to be steady and also much less sensitive to the mode than that at 1100 °C. Neither the effect of temperature nor the mode on the relative abundances of the soot-W and soot-F was significant, although the O_2/CO_2 mode gave slightly lower soot yield than the air mode. These trends, taken into consideration together with the B/N conversion as high as 97 to nearly 100% (see Table 3) and very low yields of aromatic products (Table 4) at 1200–1400 °C, formation of the soot was so fast that its yield leveled off even at 1200 °C. In addition to this, it was strongly suggested that the gasification of the soot-W simultaneously with its deposition, if any, was not significant as to cause significant temperature dependency of the soot yield and the soot-W/soot-F ratio. It was believed that the gasification of the soot-F was also insignificant if considered its residence time within the reactor. In other words, the rate of soot-W deposition was much faster than that of its gasification. Independency of the soot yield on temperature was associated with that of the gas yield. Insignificant change in the gas/soot ratio would be explained as follows. In the tubular reactor employed, the B/N vapor

experienced a temperature history obeying the temperature distribution in the axial direction that is depicted in Figure 2. Under the conditions with T_r = 1300 or 1400 °C, the B/N vapor and feed gas were heated up to T_r in the top section of the reactor, while the B/N vapor was converted to soot, gas and aromatics to a degree as substantial as that at T_r = 1200 °C. Thus, under the conditions with $C_{B/N,i}$ of 35–37 g·Nm^{-3}, the B/N conversion to soot was so fast in both the air and O_2/CO_2 modes that the conversion was nearly completed even at T_r = 1200 °C.

A number of researchers investigated homogeneous pyrolysis of hydrocarbons and reported that initial concentrations of the hydrocarbon strongly affected the rate of soot formation.[24–27] Simmons *et al.*[25] determined the rate of soot formation during the pyrolysis of rich mixtures of toluene and benzene and that of toluene/*n*-heptane mixtures by a reflected shock technique over a temperature range of 1500–1950 K and pressures of 2.6–3.6×10^5 Pa, and derived the following equation (1) where dC_f/dt and T are the rate of soot formation (unit; kg·m^{-3}·s^{-1}) and temperature (K), respectively. [C_6H_6] is the initial concentrations of benzene (mol·m^{-3}).

$$dC_f/dt = 4.7 \times 10^5 \, [C_6H_6]^{2.0} \exp(-14{,}000/T) \quad (1)$$

Rates of the soot formation from benzene under present conditions were estimated by the equation (1) assuming that the initial concentration of benzene as 0.32 mol·Nm^{-3} corresponding to 37g·Nm^{-3} B/N concentration and that benzene was converted to soot exclusively. It was then given that the soot yield reached about 70% within a second under an isothermal condition with T_r = 1200 °C. This estimation was consistent with the discussion on the results shown in Figure 3.

4.2. Influence of the Inlet Concentration of Benzene and Naphthalene on the Product Distribution.

As reported in the previous section, B/N conversion was predominated by the soot formation when the initial B/N concentration was 35–37 g·Nm^{-3}. The soot yield was not sensitive to either the temperature at T_r = 1200–1400 °C or the mode. In contrast to this, $C_{B/N,i}$ influenced the soot and gas yield significantly, and lower $C_{B/N,i}$ induced the effect of the mode on the yields. $C_{B/N,i}$ was varied from 37 to 3.7 g·Nm^{-3} at T_r = 1300 °C. The results are shown in Tables 5–6 and Figure 4. The B/N conversion was over 99.8% regardless of the mode and $C_{B/N,i}$. Figure 4 illustrates the effects of $C_{B/N,i}$ on the yields of gas, soot and tar. The tar is defined as the aromatic products and it does not include B/N.

Changing $C_{B/N,i}$ from 37 to 7 and 4 g·Nm^{-3} decreased the soot yield from 73 to 40 and 20% and from 58 to 24 and 9% in the air and O_2/CO_2 modes, respectively. Such decrease in the soot yield was compensated by increase in the gas yield. The gas was the major product at $C_{B/N,i}$ = 3.7 g·Nm^{-3}. As discussed previously, the gasification of the soot-W and soot-F was not important for their yields. The gas yields as high as 80–91% at $C_{B/N,i}$ = 3.7 g·Nm^{-3} thus resulted mainly from rapid reforming of B/N and other aromatic intermediates. It was also noted that the O_2/CO_2 mode gave clearly lower soot yield and higher gas yield than the air mode at $C_{B/N,i}$ = 3.7–7.5 g·Nm^{-3}, where the atmosphere in the O_2/CO_2 mode promoted the reforming and/or suppressed the soot formation. Suppressed soot formation by changing the mode from the air to O_2/CO_2 one was confirmed by the decrease in the yield of soot-F that was definitely formed from the vapor-phase. The soot-F/soot-W ratio seemed to be influenced by $C_{B/N,i}$, but not significantly. It was believed that the gasification of soot-W was not an important factor for the combined effects of $C_{B/N,i}$ and the mode on the soot and gas yields.

Table 6 lists the aromatic products that were detected and quantified by the GC/MS. More various types of compounds survived in the reactor at lower $C_{B/N,i}$. This was probably a result from suppressed conversion of intermediate aromatics to soot. At $C_{B/N,i}$ of 3.7 and 7.4 g·Nm^{-3}, alkylated compounds and oxygen-containing ones such as phenols, benzofuran and dibenzofuran were detected in the products. This indicated that the substitution reactions of aromatic C-H bond by hydrocarbon radicals, hydroxyl radical and other oxygen containing radicals were involved in the reforming.

4.3. Discussion on effect of mode on soot/gas formation from B/N.

For a better understanding of the effect of the mode on the gas yield, *i.e.*, the extent of reforming of B/N, the mechanism of the forming was considered employing a detailed chemical kinetic model,[28] which considered 2,216 reactions and 257 chemical species ranging from hydrogen radical to coronene, but not soot formation. This model originated from a model proposed by Richter and Howard.[29] The numerical analysis was performed by the PLUG code in the DETCHEM program package (DETHCEM ^{PLUG}).[30] The input parameters for calculation were linear velocity and chemical composition of gas at the reactor inlet, pressure and gas temperature profile through the reactor under the present experimental conditions. More details of the numerical simulation are available elsewhere.[28,31] Although the formation of soot was not considered in the analysis, the total yield of important soot precursors, *i.e.*, polyaromatic hydrocarbons (PAHs) and acetylene can be used as a semi-quantitative measure for the soot yield for the reforming in atmosphere at elevated temperature.[28]

Figure 5 compares predicted yields of soot precursors with measured yields of soot and soot precursors at T_r = 1300 °C. The soot precursors are defined as acetylene and 33 types of PAHs based on the previous study.[28] The model predicted the faster reforming of B/N in the O_2/CO_2 mode than in the air mode. The prediction was thus in agreement with the experimental result qualitatively. The under-prediction of the soot yield was attributed to no consideration of soot formation in the model. In the kinetic model employed, the extent of growth of aromatic ring systems does not occur beyond PAHs such as coronene and benzo[k]fluoranthene, which can be decomposed to smaller PAHs by the reforming. However, under the present experimental conditions, PAHs were allowed to form soot, which was gasified, if any, to a very limited degree.

Reaction pathway and sensitivity analyses were performed for selected conditions; reaction time of 0.5 s and at T_r = 1300 °C in both the air and O_2/CO_2 modes. Though details are not shown here, the reaction pathway analysis indicated that hydroxyl radical (OH·) was the most important species that caused the oxidative decomposition of B/N and other intermediate aromatics. The sensitivity analysis suggested that the following two reactions were the most important ones to form hydroxyl radical.

$$H_2O + H\cdot = H_2 + OH\cdot \quad (2)$$

$$CO_2 + H\cdot = CO + OH\cdot \quad (3)$$

Figure 6 shows predicted abundances of hydroxyl radical along the reactor axis. It is clear that the O_2/CO_2 mode can provide an atmosphere richer in the hydroxyl radical than the air mode. This prediction is consistent with the enhanced reforming and suppressed soot formation in the O_2/CO_2 mode.

The results from the experiments and the model analysis were further examined considering the range of aromatics concentration in the reducing section. As already described in

Introduction section, in the two-stage entrained-flow coal gasification, coal is injected into both the combustion and reducing sections. In the reducing section, the coal is rapidly pyrolyzed to form char, light gases and tar, which are gasified or reformed to synthesis gas. The yield of tar from the primary pyrolysis at sufficiently high temperature, if known, is available in estimating its initial concentration in the reducing section. The present authors investigated the pyrolysis of pulverized coal that had the same properties as shown in Table 1. A two-stage tubular reactor[32] was employed for rapidly pyrolyzing the coal at 900 °C, 0.2 MPa and residence time of 0.2 s, *i.e.*, with very limited degree of the secondary pyrolysis of volatiles. The tar yield from the pyrolysis was 14.9 wt%-daf-coal. In the reducing section at elevated temperature, it is believed that the initial tar undergoes aromatization by immediate thermal cracking releasing aliphatic groups and oxygen-containing groups[33], and it is further converted to gas and soot. The fraction of aromatic carbon in the initial tar was estimated by assuming that its elemental composition and carbon aromaticity of tar were equivalent with those of the parent coal.[34–38] The amount of aromatic carbon in the initial tar was estimated in this way as *ca.* 9 wt%-daf-coal.

The initial tar concentration as that of aromatic carbon in the reducing section was estimated from the above experimental result assuming that the ratio of coal injected into the reducing section to that into the combustion section was 50:50.[17] The initial tar concentration was then calculated as *ca.* 10 and 19 g-C·Nm^{-3} for the air and O_2/CO_2 modes, respectively, at T_{exit} = 1300 °C. These concentrations were thus within the range of $C_{B/N,i}$. The higher initial tar concentration in the O_2/CO_2 mode than the air mode was due to the difference in the volume of N_2 (air mode) and CO_2 (O_2/CO_2 mode) supplied to the combustion section per unit amount of coal. As shown in Table 1, it is assumed that an equivolume mixture of O_2 and CO_2 is injected

into the combustion section in the O_2/CO_2 mode, while air, *i.e.*, a 79:21 vol/vol mixture of O_2 and N_2, in the air mode.

The results shown in Figures 4–6 indicate that the O_2/CO_2 mode creates atmosphere in the reducing section more suitable to reforming of the tar to gas than the air mode does. This is, however, not necessarily a conclusion because the composition/volume of the gas fed to the gasifier and relative amounts of coal fed into the combustion/reducing sections are factors crucial for the initial concentration of tar in the reducing section.

5. Conclusion

Characteristics of gas-phase conversion of benzene and naphthalene as model tar compounds were studied with an atmospheric flow reactor at 1100–1400 °C and gaseous atmosphere simulating the reducing section of a two-stage entrained-flow coal gasifier. $C_{B/N,i}$ in the range of 3.7–37 g·Nm^{-3} strongly influenced the fate of B/N. Decreasing $C_{B/N,i}$ made the reforming of B/N to gas more important, suppressing the soot formation. Compared with the air mode, the O_2/CO_2 mode created atmosphere richer in hydroxyl radical and other species most reactive with B/N, and promoted the reforming of B/N to gas at lower $C_{B/N,i}$.

Author Information

*Telephone: +81-92-583-7796 Fax: +81-92-583-7793

E-mail: junichiro_hayashi@cm.kyushu-u.ac.jp

Acknowledgement

A part of this work was carried out in R&D project that was financially supported by the New Energy and Industrial Technology Development Organization (NEDO), Japan. The authors are also grateful to a grant from the Global-Centre of Excellence in Novel Carbon Resource Sciences (NCRS; Kyushu University), and Japan Society for the Promotion of Science (JSPS; Grant-in-Aid for JSPS Fellows, Grant Number 24·56512).

References

(1) Araki, S. R&D of an IGCC system by the 200 t/d pilot plant at Nakoso. *Proceedings of APEC Third Technical Seminar on Clean Coal Technology*, Taejon, Korea, August 29–31, 1995.

(2) Kaneko, S.; Ishibashi, Y.; Wada, J. Project Status of 250 MW Air-blown IGCC Demonstration Plant. Presented at 2002 Gasification Technologies Conference, San Francisco, California, USA, October 28–30, 2002.

(3) Jaeger, H. Japan 250 MW Coal Based IGCC Demo Plant Set for 2007 Start–Up. *Gas Turbine World*, 35 (2), 2005, 12–15.

(4) Sakamoto, K. Commercialization of Mitsubishi's IGCC/Gasification Technology. Presented at 2011 Gasification Technologies Conference; San Francisco, California, USA, October 9–12, 2011.

(5) Shirai, H.; Hara, S.; Koda, E.; Watanabe, H.; Yoshiba, F.; Inumaru, J.; Nunokawa, M.; Makino, H.; Mimaki, T.; Abe, T. *Proposal of the high efficient system with CO_2 capture and the task on an integrated coal gasification combined cycle power generation*; Central Research Institute of Electric Power Industry (CRIEPI): Japan, 2007; Energy Engineering Research Laboratory Report M07003

(6) Kidoguchi, K.; Hara, S.; Oki, Y.; Kajitani, S.; Umemoto, S.; Umetsu, H. *Development of High Thermal Efficiency IGCC with CO_2 Capture–Experimental Examination on Effect of Gasification Reaction Promotion by CO_2 Enriched Using Bench Scale Gasifier Facility–*; Central Research Institute of Electric Power Industry (CRIEPI): Japan, 2011; Energy Engineering Research Laboratory Report M10016

(7) Hayashi, J.-i. Breaking through Rate/Temperature Limitations in Gasification of Carbon Resources, G-COE Program Kyushu University Novel Carbon Resource Sciences Newsletter, 2011, *5*, 13–16 (ISSN: 1884-6297)

(8) Giuffrida, A.; Romano, M. C.; Lozza, G. *Appl. Energy* 2011, *88*, 3949–3958

(9) Takarada, T.; Tamai, Y.; Tomita, A. *Fuel* 1985, *64*, 1438–1442

(10) Miura, K.; Hashimoto, K.; Silveston, P. L. *Fuel* 1989, *68*,1461–1475

(11) Lizzio, A. A.; Jiang, H.; Radovic, L. R. *Carbon* 1990, *28*, 7–19

(12) Kajitani, S.; Hara, S.; Matsuda, H. *Fuel* 2002, *81*, 539–546

(13) Jamil, K.; Hayashi, J.-i.; Li, C.-Z. *Fuel* 2004, *83*, 833–843

(14) Bayarsaikhan, B.; Hayashi, J.-i.; Shimada, T.; Sathe, C.; Li, C.-Z.; Tsutsumi, A.; Chiba, T. *Fuel* 2005, *84*, 1612–1621

(15) Roberts, D. G.; Harris, D. J. *Fuel* 2007*, 86,* 2672–2678

(16) Chen, J. C.; Castagnoli, C.; Niksa, S. *Energy Fuels* 1992, *6*, 264–271

(17) Watanabe, H.; Otaka, M. *Fuel* 2006, *85*, 1935–1943

(18) Takase, S.; Koyama, T.; Yokohama, K.; Ito, K.; Ishii, H. (Mitsubishi Heavy Industries, Ltd., Japan). Jpn. Kokai Tokkyo Koho JP 2008150463, 2008.

(19) Garcia, X. A.; Hüttinger, K. J. *Fuel* 1989, *68*, 1300–1310

(20) Kurkela, E.; Ståhlberg, P. *Fuel Process. Technol.* 1992, *31*, 1–21

(21) Milne, T. A.; Evans, R. J. Biomass Gasifier "Tars": Their Nature, Formation and Conversion; NREL/TP-570−25357; National Renewable Energy Laboratory: Golden, CO, 1998.

(22) Ishibashi, Y.; Shinada, O. First Year Operation Results of CCP's Nakoso 250 MW Air-Blown IGCC Demonstration Plant. Presented at 2008 Gasification Technologies Conference; Washington, D.C., Washington, USA, October 5–8, 2008

(23) Hashimoto, T.; Sakamoto, K.; Kitagawa, Y.; Hyakutake, Y.; Setani, N. Development of IGCC commercial plant with air-blown gasifier. Mitsubishi Heavy Industries Technical Review, 46 (2), June; 2009

(24) Wang, T. S.; Matula, R. A.; Farmer, R. C. *Proceedings of the Eighteenth Symposium (International) on Combustion*; The Combustion Institute: Pittsburgh, PA, 1981; 1149–1158

(25) Simmons, B.; Williams, A. *Combust. Flame* 1988, *71*, 219–232

(26) Shurupov, S. V. *Proc. Combust. Inst.* 2000, *28*, 2507–2514

(27) Agafonov, G. L.; Vlasov, P. A.; Smirnov, V. N. *Kinet. Catal.* 2011, *52*, 358–370

(28) Norinaga, K.; Sakurai, Y.; Sato, R.; Hayashi, J.-i. *Chem. Eng. J.* 2011, *178*, 282–290

(29) Richter, H.; Howard, J. B. *Phys. Chem. Chem. Phys.* 2002, *4*, 2038–2055

(30) DETCHEM Software package, www.detchem.com

(31) Norinaga, K.; Janardhanan, V. M.; Deutschmann, O. *Int. J. Chem. Kinet.* 2008, 40, 199–208

(32) Norinaga, K.; Shoji, T.; Kudo, S.; Hayashi, J.-i. Detailed chemical kinetic modelling of vapour-phase cracking of multi-component molecular mixtures derived from the fast pyrolysis of cellulose. Fuel 2011; doi:10.1016/j.fuel.2011.07.045, in press.

(33) Hayashi, J.-i.; Takahashi, H.; Iwatsuki, M.; Essaki, K.; Tsutsumi, A.; Chiba, T. *Fuel* 2000, *79*, 439–447

(34) Freihaut, J. D.; Proscia, W. M.; Seery, D. J. *Energy Fuels* 1989, *3*, 692–703

(35) Fletcher, T. H.; Solum, M. S.; Grant, D. M.; Critchfield, S.; Pugmire, R. J. *Proceedings of the Twenty-Third Symposium (International) on Combustion*; The Combustion Institute: Pittsburgh, PA, 1990; 1231–1237

(36) Watt, M.; Fletcher, T. H.; Bai, S.; Solum, M. S.; Pugmire, R. J. *Proceedings of the Twenty-Sixth Symposium (International) on Combustion*; The Combustion Institute: Pittsburgh, PA, 1996; 3153–3160

(37) Kidena, K.; Murata, S.; Nomura, M. *Energy Fuels* 1996, *10*, 672–678

(38) Kidena, K.; Murata, S.; Artok, L.; Nomura, M. *J. Jpn. Inst. Energy* 1999, *78*, 869–876

Table 1. Assumptions in numerical simulation of gasification.

Temperature	
• Combustor inlet (air or O_2/CO_2)	200 °C
• Combustor exit (syngas)	1800 °C
• Reductor inlet (coal)	25 °C
• Reductor exit (syngas), T_{exit}	variable
Heat loss	3% of coal's LHV
O_2/CO_2 ratio at combustor inlet	50/50 mol·mol^{-1}
Coal (Datong coal)	
• Moisture content	5.0 wt%-wet
• Ash content	0
• ΔH_f° of coal	–7.3 kJ·mol-C^{-1}
• C, H and O contents	84.6, 5.2 and 9.1 wt%-dry
Others	
• Absence of char, soot, tar and lower hydrocarbons at the combustor exit	
• Absence of tar and lower hydrocarbons in syngas at the reductor exit	
• Chemical equilibrium of syngas (water-gas shift reaction)	

Table 2. Numerically derived compositions of the product gas at gasifier exit in air- and O_2/CO_2-blown modes.

	Air-blown mode				O_2/CO_2-blown mode			
T_r, °C	1100	1200	1300	1400	1100	1200	1300	1400
Feed gas composition, vol%								
CO	30.0	28.1	26.2	24.2	63.4	62.4	61.3	60.0
CO_2	1.36	2.20	3.02	3.87	14.3	15.5	16.8	18.2
H_2	11.7	10.4	9.02	7.59	15.4	13.9	12.4	11.0
H_2O	1.07	1.95	2.90	3.87	6.94	8.25	9.51	10.7
N_2	55.8	57.3	58.8	60.4	Null	Null	Null	Null

Table 3. Carbon distribution among products (gas, soot and tar) and unconverted benzene/naphthalene at $C_{B/N,i}$ = 35–37 g·Nm^{-3}.

	Air-blown mode				O_2/CO_2-blown mode			
T_r, °C	1100	1200	1300	1400	1100	1200	1300	1400
Inlet concentration of benzene/naphthalene, g·Nm^{-3}	36.3	35.7	36.8	36.2	36.1	36.1	36.8	35.4
Yield of products and unconverted benzene/naphthalene, %-C								
Gas	4.34	27.3	27.1	31.6	16.0	30.3	36.7	33.3
Soot	66.6	69.8	72.8	67.3	52.2	69.2	63.1	66.7
Tar (except for benzene/naphthalene)	6.40	0.15	0.01	<0.01	3.80	0.11	<0.01	<0.01
Benzene (initial; 70%)	18.0	0.12	<0.01	0.04	23.0	<0.01	<0.01	<0.01
Naphthalene (initial; 30%)	4.64	2.59	0.05	1.07	4.95	0.37	0.16	0.02
Overall benzene/naphthalene conversion, %-C	77.3	97.3	>99.9	98.9	72.1	99.6	99.8	>99.9

Table 4. Yields of tar components in air- and O_2/CO_2-blown modes at $C_{B/N,i}$ = 35–37 g·Nm^{-3}.

	Air-blown mode				O_2/CO_2-blown mode			
T_r, °C	1100	1200	1300	1400	1100	1200	1300	1400
Inlet concentration of benzene/naphthalene, g·Nm^{-3}	36.3	35.7	36.8	36.2	36.1	36.1	36.8	35.4
Yield of compounds in tar, %-C								
Toluene	8.5×10^{-3}	–	–	–	2.4×10^{-2}	4.1×10^{-4}	–	1.5×10^{-3}
Ethylbenzene	–	–	2.9×10^{-4}	–	–	–	–	–
Styrene	2.6×10^{-2}	1.3×10^{-2}	5.5×10^{-4}	–	0.31	7.3×10^{-3}	–	–
Phenol	1.1×10^{-3}	–	–	–	3.6×10^{-2}	4.9×10^{-3}	–	–
Indene	5.5×10^{-2}	1.5×10^{-2}	–	–	0.43	1.5×10^{-2}	–	–
Naphthalene, 2-methyl-	2.5×10^{-4}	–	–	–	2.8×10^{-3}	–	–	–
Naphthalene, 1-methyl-	6.0×10^{-5}	–	–	–	3.5×10^{-3}	–	–	–
Biphenyl	3.0×10^{-2}	8.1×10^{-5}	4.3×10^{-4}	–	0.13	4.0×10^{-5}	2.5×10^{-4}	–
Acenaphthylene	5.2	9.2×10^{-2}	1.3×10^{-2}	1.2×10^{-3}	1.2	3.7×10^{-2}	4.1×10^{-4}	2.7×10^{-5}
2-Naphthalenol (2-Naphthol)	–	–	–	2.9×10^{-5}	–	–	–	–
Dibenzofuran	–	–	–	–	4.2×10^{-5}	–	–	–
Phenanthrene	0.12	7.4×10^{-3}	7.4×10^{-5}	5.1×10^{-4}	0.28	2.9×10^{-3}	4.2×10^{-5}	9.7×10^{-5}
Anthracene	4.3×10^{-3}	1.5×10^{-4}	–	3.4×10^{-4}	1.0×10^{-2}	4.7×10^{-5}	–	–
Fluoranthene	0.54	7.8×10^{-3}	3.0×10^{-4}	1.2×10^{-3}	0.69	4.3×10^{-3}	3.0×10^{-4}	1.7×10^{-4}
Pyrene	0.40	1.8×10^{-2}	3.6×10^{-4}	2.7×10^{-3}	0.70	3.7×10^{-2}	3.6×10^{-4}	1.4×10^{-4}

Table 5. Carbon distribution among the products (gas, soot and tar) and unconverted benzene/naphthalene in air- and O_2/CO_2-blown modes at T_r = 1300 °C.

	Air-blown mode			O_2/CO_2-blown mode		
Inlet concentration of benzene/naphthalene, g·Nm^{-3}	3.72	7.43	36.8	3.70	7.49	36.8
Yield of products and unconverted benzene/naphthalene, %-C						
Gas	80.2	59.8	27.1	90.9	75.5	36.7
Soot	19.8	40.2	72.8	9.08	24.4	63.1
Tar (except for benzene/naphthalene)	0.02	0.03	0.01	0.02	0.03	<0.01
Benzene (initial; 70%)	<0.01	<0.01	<0.01	<0.01	<0.01	<0.01
Naphthalene (initial; 30%)	<0.01	0.01	0.05	<0.01	0.05	0.16
Overall benzene/naphthalene conversion, %-C	>99.9	>99.9	>99.9	>99.9	>99.9	99.8

Table 6. Yields of tar components in air- and O_2/CO_2-blown modes at T_r = 1300 °C.

	Air-blown mode			O_2/CO_2-blown mode		
Inlet concentration of benzene/naphthalene, g·Nm^{-3}	3.72	7.43	36.8	3.70	7.49	36.8
Yield of compounds in tar, %-C						
Toluene	3.0×10^{-4}	5.5×10^{-4}	–	1.7×10^{-2}	1.6×10^{-4}	–
Ethylbenzene	2.5×10^{-4}	–	2.9×10^{-4}	–	7.1×10^{-4}	–
Styrene	3.2×10^{-4}	1.6×10^{-4}	5.5×10^{-4}	2.2×10^{-4}	3.8×10^{-4}	–
Benzene, 1,2-dimethyl- (*o*-Xylene)	1.1×10^{-4}	7.8×10^{-5}	–	1.8×10^{-4}	2.0×10^{-4}	–
Phenol	6.6×10^{-3}	8.2×10^{-3}	–	1.1×10^{-2}	1.3×10^{-2}	–
Phenol, 2-methyl- (*o*-Cresol)	3.0×10^{-3}	2.2×10^{-3}	–	2.3×10^{-3}	1.5×10^{-3}	–
Phenol, 3-methyl- (*m*-Cresol)	4.8×10^{-3}	5.8×10^{-3}	–	5.2×10^{-3}	5.6×10^{-3}	–
Benzofuran	1.2×10^{-4}	1.4×10^{-4}	–	1.6×10^{-4}	1.8×10^{-4}	–
Indene	6.7×10^{-5}	1.7×10^{-4}	–	4.5×10^{-4}	3.1×10^{-4}	–
Phenol, 2-methoxy- (*o*-Guaiacol)	–	–	–	–	2.6×10^{-4}	–
Phenol, 2,6-dimethyl- (2,6-Xylenol)	2.6×10^{-4}	2.0×10^{-4}	–	4.8×10^{-4}	9.0×10^{-4}	–
Phenol, 2,4-dimethyl- (2,4-Xylenol)	3.4×10^{-4}	3.6×10^{-4}	–	–	8.9×10^{-4}	–
1,3-Benzenediol (Resorcinol)	8.4×10^{-4}	6.5×10^{-5}	–	–	2.5×10^{-3}	–
3,5-Dihydroxytoluene (Orcinol)	4.5×10^{-4}	1.4×10^{-4}	–	5.9×10^{-4}	9.2×10^{-4}	–
Phenol, 2-methoxy-4-methyl-	4.8×10^{-4}	3.9×10^{-4}	–	2.5×10^{-4}	4.3×10^{-4}	–
Naphthalene, 2-methyl-	6.5×10^{-5}	9.4×10^{-5}	–	1.2×10^{-4}	1.6×10^{-3}	–
Naphthalene, 1-methyl-	1.8×10^{-4}	1.1×10^{-4}	–	1.7×10^{-4}	7.1×10^{-5}	–
Biphenyl	7.0×10^{-6}	3.7×10^{-4}	4.3×10^{-4}	7.8×10^{-6}	1.1×10^{-3}	2.5×10^{-4}
Acenaphthylene	3.9×10^{-5}	4.5×10^{-4}	1.3×10^{-2}	1.3×10^{-5}	1.4×10^{-3}	4.1×10^{-4}
1-Naphthalenol (1-Naphthol)	3.7×10^{-4}	9.3×10^{-5}	–	1.2×10^{-4}	2.6×10^{-4}	–
2-Naphthalenol (2-Naphthol)	2.6×10^{-4}	1.6×10^{-4}	–	3.8×10^{-4}	5.8×10^{-4}	–
Dibenzofuran	–	1.2×10^{-4}	–	5.1×10^{-5}	–	–
Phenanthrene	1.6×10^{-5}	8.2×10^{-5}	7.4×10^{-5}	5.4×10^{-5}	1.7×10^{-4}	4.2×10^{-5}
Anthracene	–	1.1×10^{-4}	–	6.2×10^{-5}	–	–
Fluoranthene	3.4×10^{-5}	1.4×10^{-4}	3.0×10^{-4}	3.2×10^{-4}	8.1×10^{-4}	3.0×10^{-4}
Pyrene	6.3×10^{-4}	7.6×10^{-4}	3.6×10^{-4}	1.4×10^{-4}	1.1×10^{-4}	3.6×10^{-4}

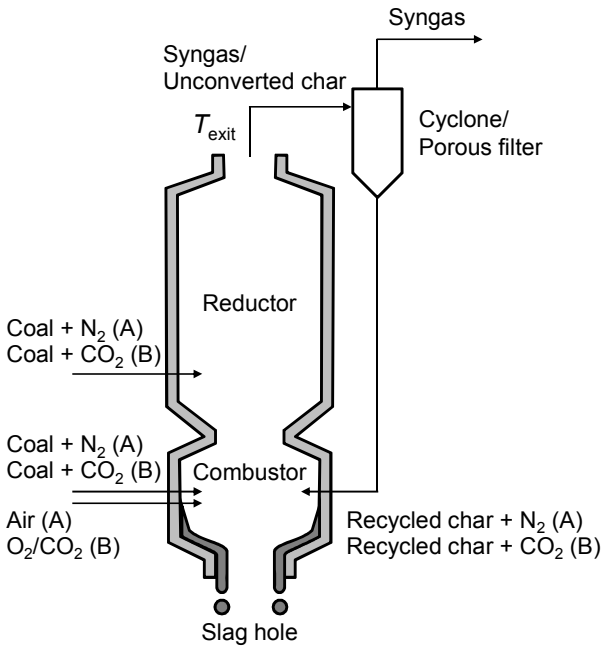

Figure 1. Schematic diagram of two-stage entrained-flow coal gasifier for (A) air-blown gasification and (B) O_2/CO_2-blown gasification.

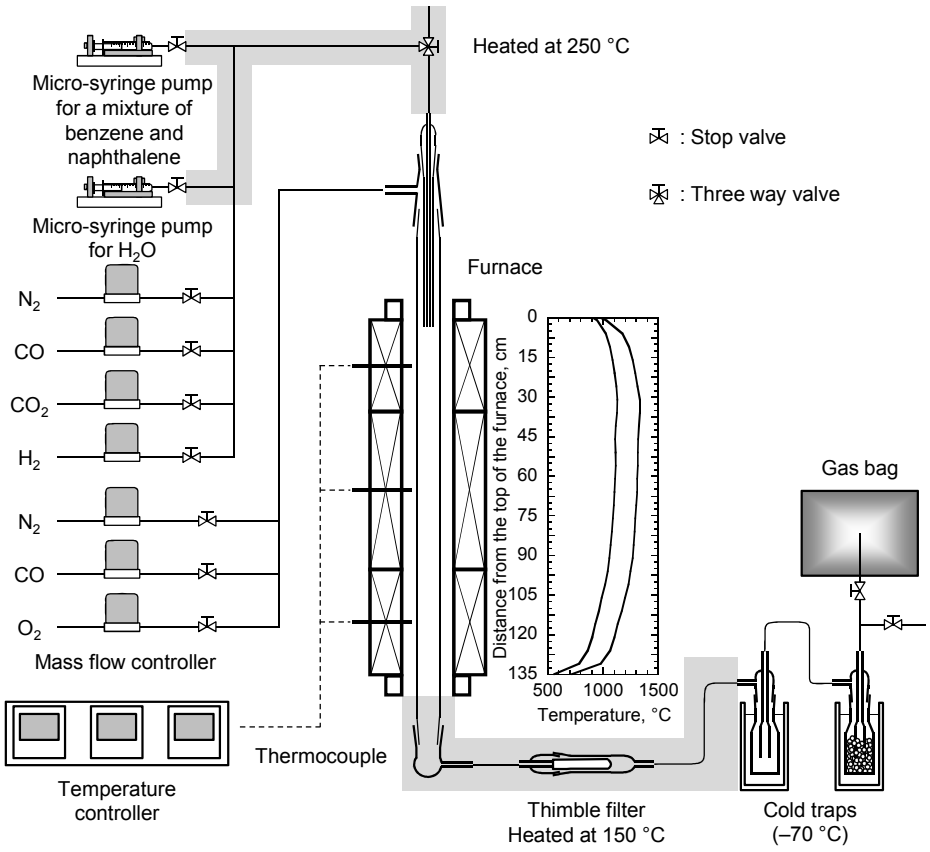

Figure 2. Schematic diagram of experimental apparatus.

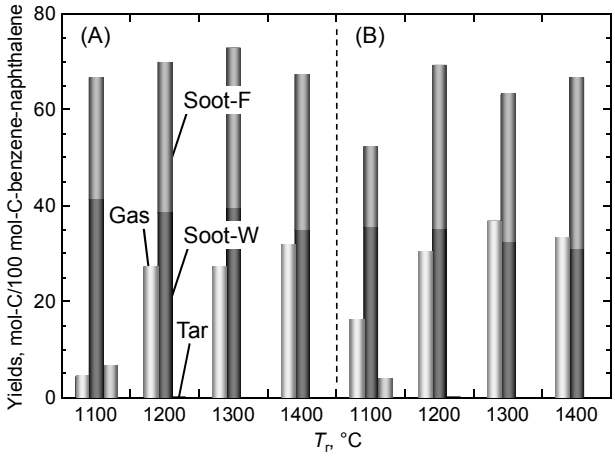

Figure 3. Yields of soot, gas, and tar (except for benzene/naphthalene) at $C_{B/N,i}$ = 35–37 g·Nm^{-3} in (A) air-blown mode and (B) O_2/CO_2-blown mode.

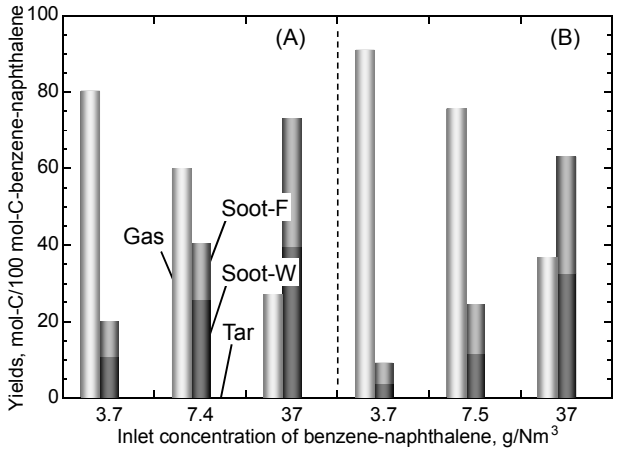

Figure 4. Yields of soot, gas, and tar (except for benzene/naphthalene) at T_r = 1300 °C in (A) air-blown mode and (B) O_2/CO_2-blown mode.

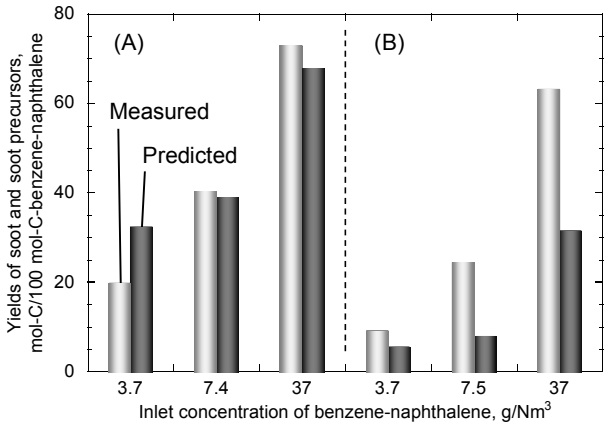

Figure 5. Comparison between measured and predicted values of total yields of soot and soot precursors at T_r = 1300 °C in (A) air-blown mode and (B) O_2/CO_2-blown mode.

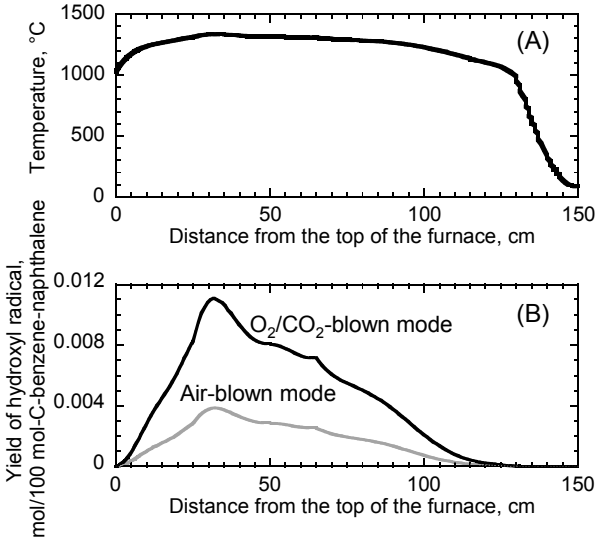

Figure 6. Numerically derived yield of hydroxyl radical along the reactor axis; (A) measured axial temperature distribution of the reactor and (B) yield of hydroxyl radical at T_r = 1300 °C and $C_{B/N,i}$ = 3.7 g·Nm^{-3} in air- and O_2/CO_2-blown modes.